nature water

Article https://doi.org/10.1038/s44221-023-00128-y

Future increases in Amazonia water stress from CO_2 physiology and deforestation

In the format provided by the authors and unedited

Supplementary Figures and Tables

7 figures, 3 tables

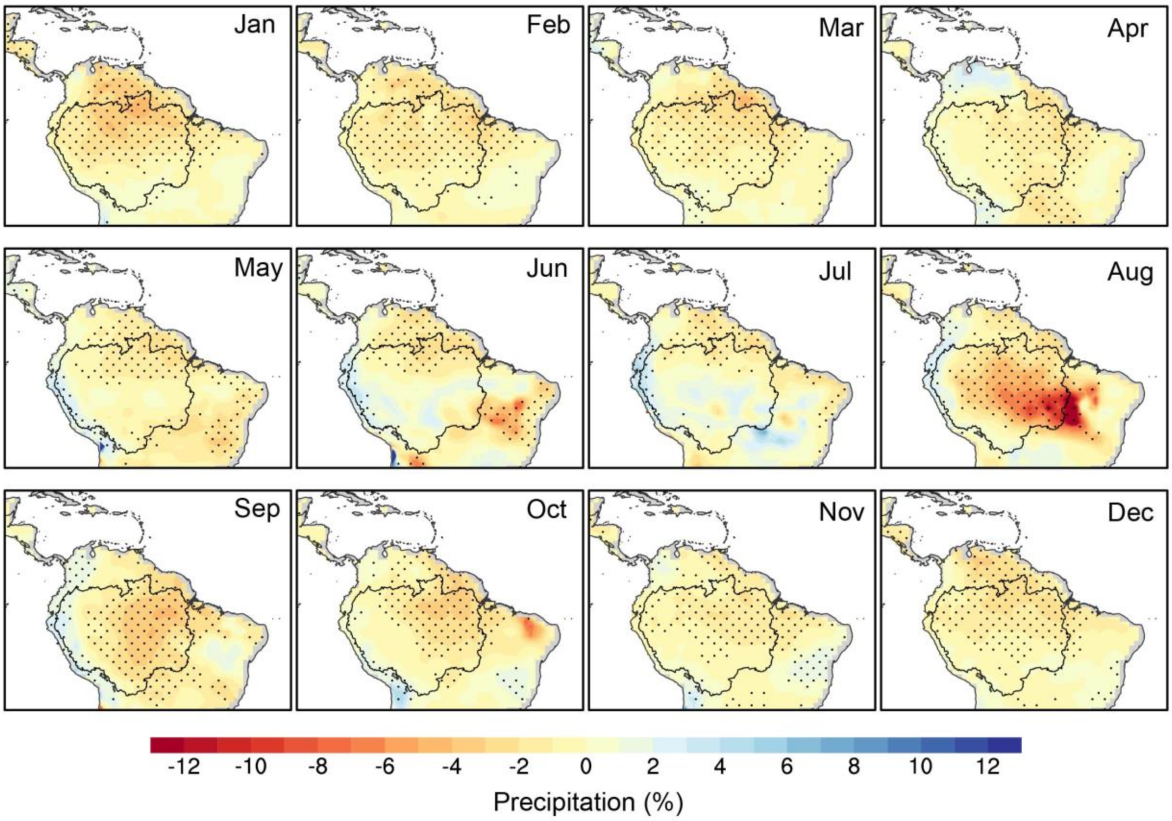

Supplementary Fig. 1. Intra-annual patterns of precipitation response to 100 ppm increase in CO_2 concentration. For each month, linear regressions were performed for precipitation at each pixel against the atmospheric CO_2 concentration from their 140-year simulations of the C4MIP experiments (see Methods). Dotted area indicates the model agreement, with at least six out of eight models agreeing on the sign of the precipitation response.

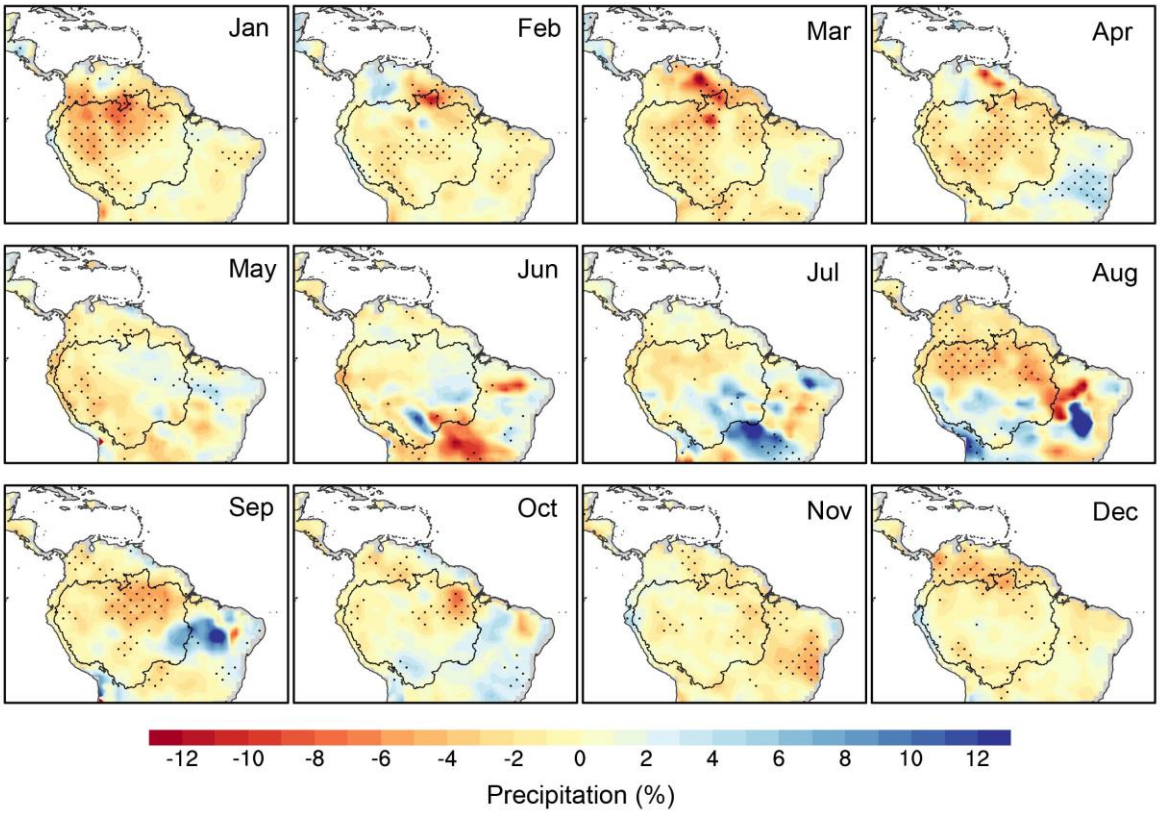

Supplementary Fig. 2. Intra-annual patterns of precipitation response to 10% deforestation in the Amazon basin. For each month, linear regressions were performed for precipitation at each pixel against the basin-scale average in deforestation fraction from their 50-year simulations of the LUMIP experiments (see Methods). Dotted area indicates the model agreement, with at least six out of eight models agreeing on the sign of the precipitation response.

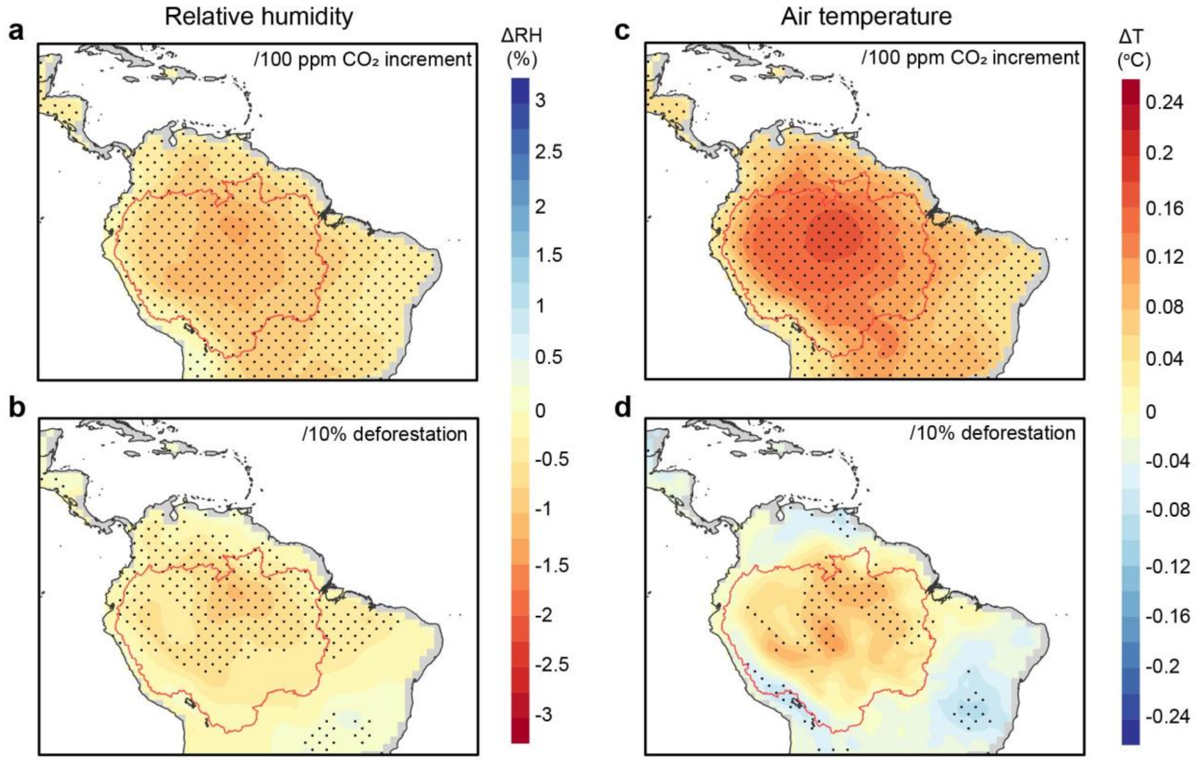

Supplementary Fig. 3. Same as Fig. 2 but for (**a**), (**b**) surface relative humidity (RH) and (**c**), (**d**) air temperature (T). Dotted area for (**c**), (**d**) indicates the model agreement, with at least six out of eight models agreeing on the sign of the multi-model average T response. Due to the limited model output for RH, the dotted area for (**a**), (**b**) indicates at least three out of available model output agreeing on the sign of the multi-model average RH response.

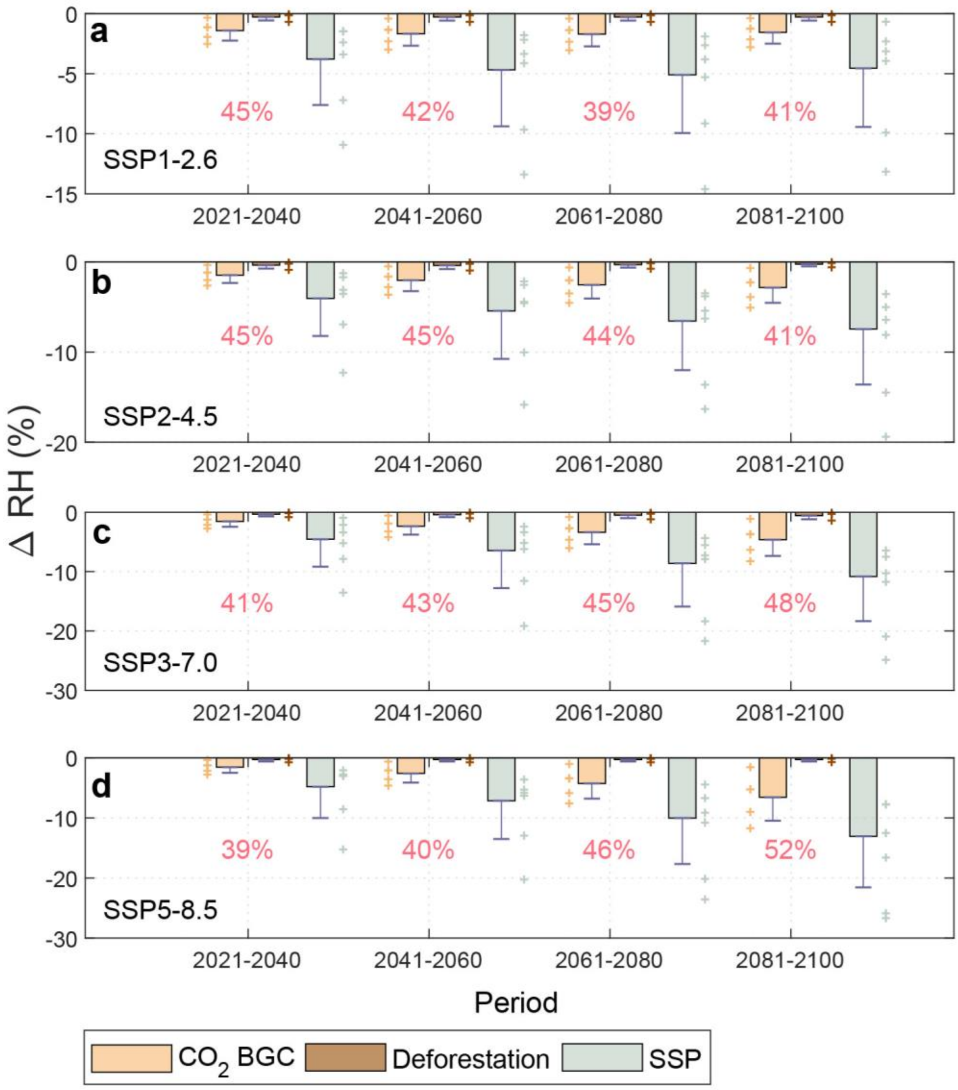

Supplementary Fig. 4. Same as Fig. 4 but for surface relative humidity (RH, %). Each error bar indicates 1 standard deviation (SD) being added to the mean values across the CMIP6 models with available output (n = 5 for CO_2 physiology, n = 6 for SSP simulation, and n = 4 for deforestation). Data point for each model has been shown along with the bar as indicated by plus sign.

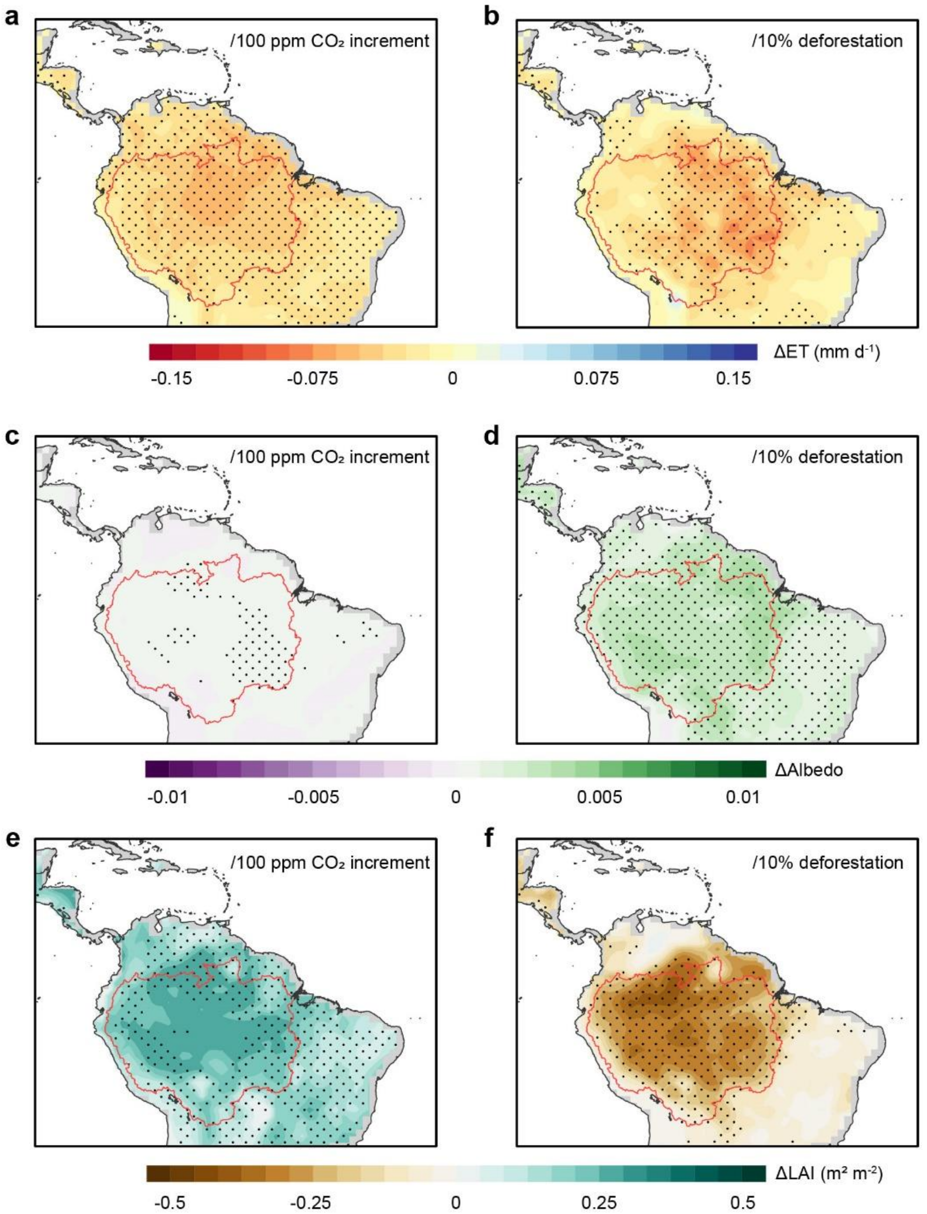

Supplementary Fig. 5. Same as Figure 2 but for three mechanism variables such as evapotranspiration (ET), surface albedo, and leaf area index (LAI) in response to either CO_2 physiological effects or deforestation in each idealized experiment. Dotted area indicates the model agreement, with at least six out of seven (**a**), six out of eight (**b**), six out of six (**c**), six out of seven (**d**), four out of five (**e**), and six out of seven (**f**) models agreeing on the sign of the multi-model mean mechanism variables response. ET is not available from IPSL-CM6A-LR in 1pctCO2-bgc experiment. Albedo is calculated from surface upwelling and downwelling shortwave radiation assuming clear sky, which is not available from IPSL-CM6A-LR and UKESM1-0-LL in 1pctCO2-bgc experiment and from MPI-ESM1-2-LR in deforest-glob experiment. LAI is not available from CanESM2, IPSL-CM6A-LR, UKESM1-0-LL in 1pctCO2-bgc experiment and from UKESM1-0-LL in deforest-glob experiment. Though the LAI increases in response to CO_2 fertilization in panel (**e**), the reduction in transpiration from stomatal closure dominates the total ET decline in panel (**a**).

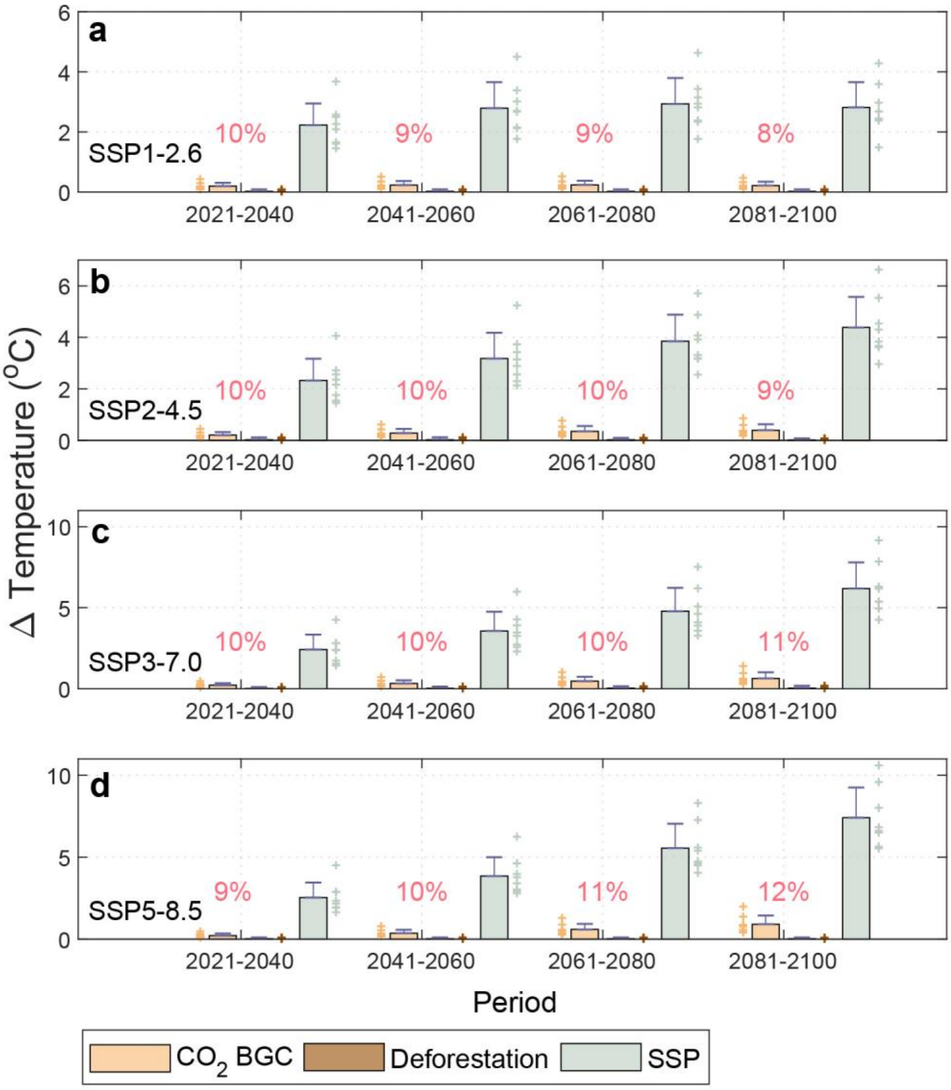

Supplementary Fig. 6. Same as Fig. 4 but for surface air temperature (°C). Each error bar indicates 1 standard deviation (SD) being added to the mean values across the CMIP6 models with available output (n = 8 for CO_2 physiology and SSP simulation, and n = 6 for deforestation). Data point for each model has been shown along with the bar as indicated by plus sign.

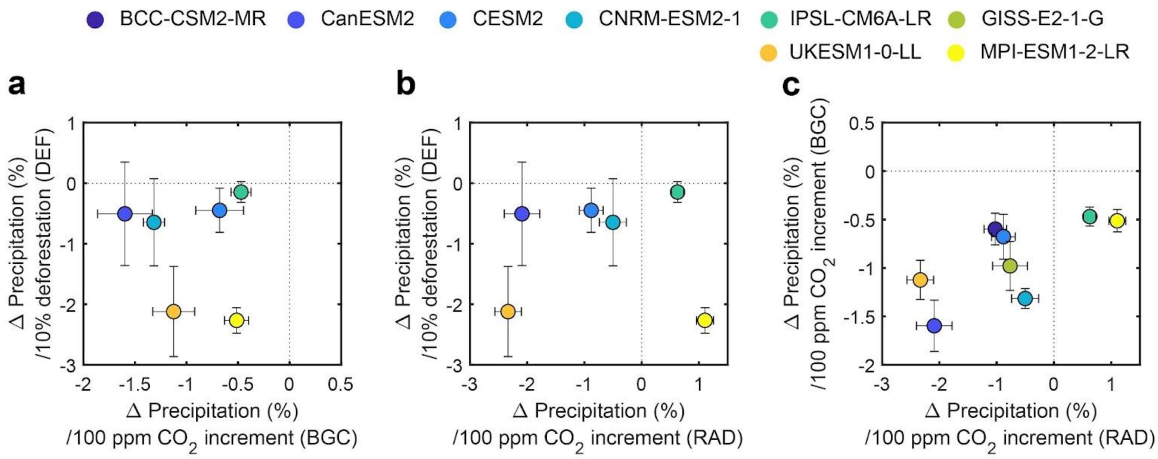

Supplementary Fig. 7. Cross-model scatter plot showing the Amazonian precipitation response (in percent change) to deforestation, CO_2 physiology (BGC), and CO_2 radiative forcing (RAD). The precipitation sensitivity was computed from a linear regression, in which the precipitation was regarded as a function of deforestation fraction in the LUMIP deforest-glob experiments (DEF), of CO_2 concentrations in the C4MIP 1pctCO2-bgc experiments (BGC), and of CO_2 concentrations in the C4MIP 1pctCO2-rad experiments (RAD). The error bar indicates 1 standard error (SE) being added to the regression slope by t-test against CO_2 in BGC ($n = 140$) and RAD ($n = 140$), and against deforestation in DEF ($n = 50$). This analysis suggests that the deforestation effect on precipitation is largely independent of the CO_2 physiology effect within the set of models we evaluated, as shown in panel A. A weak relationship does exist between the strength of the precipitation response to forcing from CO_2 physiology and the response to forcing from CO_2 radiative effects (panel c; $R = 0.70$; $P = 0.05$).

Table S1. Description of each CMIP6 model used in this study.

Model	Model center	Model resolution	C4MIP ensemble number	LUMIP ensemble number
BCC-CSM2-MR	Beijing Climate Center, China	320 × 160 (1.125° × 1.125°)	1	1
CanESM5	Canadian Centre for Climate Modelling and Analysis, Canada	128 × 64 (2.8° × 2.8°)	1	1
CESM2	National Center for Atmospheric Research, USA	288 × 192 (1.25° × 0.94°)	1	3
CNRM-ESM2-1	Centre National de Recherches Météorologiques, France	256 × 128 (1.4° × 1.4°)	4	1
IPSL-CM6A-LR	Institut Pierre-Simon Laplace, France	144 × 143 (2.5° × 1.27°)	1	3
GISS-E2-1-G	NASA Goddard Institute for Space Studies, USA	144 × 90 (2.5° × 2°)	1	1
UKESM1-0-LL	Met Office Hadley Centre, UK	192 × 144 (1.87° × 1.25°)	1	1
MPI-ESM1-2-LR	Max Planck Institute for Meteorology, Germany	192 × 96 (1.9° × 1.9°)	3	7

Table S2. Regression for each model regarding the mean annual precipitation, surface relative humidity, and air temperature response to 100 ppm CO_2 increase via the plant physiological effects and 10% deforestation in the Amazon basin. Regression results of precipitation and air temperature response to deforestation are not applied for BCC-CSM2-MR and GISS-E2-1-G due to the unavailability of tree cover fraction output. Models without a relative humidity response to both CO_2 increase and deforestation are lack of available output of the relative humidity and are indicated as NA.

Model	Response to 100 ppm CO_2 increase			Response to 10% deforestation		
	Precipitation (%)	**Surface relative humidity (%)**	**Surface air temperature (°C)**	**Precipitation (%)**	**Surface relative humidity (%)**	**Surface air temperature (°C)**
BCC-CSM2-MR	-0.60 ± 0.16*	NA	0.06 ± 0.01*	NA	NA	NA
CanESM5	-1.60 ± 0.26*	-0.73 ± 0.10*	0.12 ± 0.02*	-0.51 ± 0.85	-0.10 ± 0.28	-0.01 ± 0.06
CESM2	-0.68 ± 0.23*	-0.22 ± 0.04*	0.06 ± 0.01*	-0.45 ± 0.36	NA	0.15 ± 0.02*
CNRM-ESM2-1	-1.32 ± 0.10*	NA	0.08 ± 0.01*	-0.65 ± 0.72	NA	0.03 ± 0.05
IPSL-CM6A-LR	-0.47 ± 0.10*	-1.25 ± 0.04*	0.19 ± 0.01*	-0.15 ± 0.17	-0.32 ± 0.06*	0.05 ± 0.02*
GISS-E2-1-G	-0.98 ± 0.25*	NA	0.11 ± 0.03*	NA	NA	NA
UKESM1-0-LL	-1.12 ± 0.20*	-1.62 ± 0.06*	0.28 ± 0.02*	-2.12 ± 0.74*	-0.22 ± 0.22	-0.19 ± 0.06*
MPI-ESM1-2-LR	-0.51 ± 0.12*	-0.73 ± 0.03*	0.11 ± 0.01*	-2.27 ± 0.21*	-1.14 ± 0.07*	0.10 ± 0.02*

* indicate a significance level of $P < 0.05$ for regression coefficients computed to represent the climate response to rising CO_2 and deforestation fraction.

Table S3. Future projection in Amazonian precipitation (%) by 2081-2100 under four different Shared Socioeconomic Pathways (SSP) for each model used in this study. The relative precipitation is calculated as the mean precipitation during 2081-2100 as compared to the climatological precipitation from the pre-industrial levels (i.e., 1850).

Model name	SSP1-2.6	SSP2-4.5	SSP3-7.0	SSP5-8.5
BCC-CSM2-MR	-11.72	-13.61	-17.81	-20.43
CanESM2	-15.97	-23.01	-29.41	-29.81
CESM2	-4.50	-6.01	-13.12	-16.25
CNRM-ESM2-1	0.35	-1.00	-7.62	-11.14
IPSL-CM6A-LR	4.33	2.39	3.86	3.12
GISS-E2-1-G	-7.24	-11.24	-22.16	-10.09
UKESM1-0-LL	-8.58	-11.56	-18.00	-19.01
MPI-ESM1-2-LR	8.23	1.96	1.12	-5.58